33RD INTERNATIONAL COSMIC RAY CONFERENCE, RIO DE JANEIRO 2013
THE ASTROPARTICLE PHYSICS CONFERENCE

ICRC 2013

Model Independent Search For GRB Neutrinos Interacting Inside IceCube

THE ICECUBE COLLABORATION[1],

[1] *See special section in these proceedings*

jcasey8@gatech.edu

Abstract: IceCube is a km-scale neutrino detector operating at the geographical South Pole. It is sensitive to high energy neutrinos. Many GRB models predict the generation of high energy neutrinos through various hadronic interactions at different stages of the burst such as the prompt phase, the early afterglow and/or a precursor phase. A potential neutrino lightcurve, however, remains unknown. We report a search of temporal and spatial correlation between neutrinos and a stacked list of GRBs on a time scale from $\pm$10 s to $\pm$15 days. Previous searches by IceCube that study correlations up to $\pm$1 day have focused on through-going tracks from muon neutrinos. As neutrino candidates we use the 28 events found between $\approx$30 TeV and $\approx$1.2 PeV using the high-energy starting event technique. This method is sensitive to neutrinos of all flavors over 4π sr. The temporal and spatial correlation method reported here uses a likelihood ratio test. We search for correlations of neutrino events with 562 GRBs reported mostly by Fermi GBM and Swift BAT from May 2010 to May 2012.

Corresponding authors: James Casey[1], Ignacio Taboada[1]
[1] *Center for Relativistic Astrophysics & School of Physics. Georgia Institute of Technology, Atlanta, USA*

Keywords: Neutrino, Gamma Ray Bursts, IceCube

1 Introduction

Gamma Ray Bursts (GRBs) have been suggested as sources for the highest-energy cosmic rays [1]. If this hypothesis is correct, neutrinos should also be produced [2, 3, 4]. Since neutrinos are neutral particles, they are not deflected by magnetic fields and point back to the sources of the highest energy cosmic rays. Several models predict the neutrino fluence to be sufficiently large to be detectable by the IceCube Neutrino Observatory. Previous searches with IceCube have failed to find a temporal and spatial correlation between GRBs and neutrinos. As a result, IceCube has been able to exclude those models in which GRBs are the only sources of the highest energy cosmic rays and the cosmic rays escape as neutrons [5]. Previous searches in IceCube looked for through-going tracks from ν_μ interactions, spatially correlated with bursts, and within $\pm$1 day of the burst ('model-independent') or during the keV–MeV gamma ray emission and assuming a hard signal spectrum ('model-dependent').

The null result reported by IceCube has triggered a revision of theoretical predictions of neutrino emission by GRBs. Present models have improvements, such as a more detailed particle physics simulation, that reduce the signal expectation in IceCube by about one order of magnitude [6]. However these updated models should still be within the reach of IceCube with a few years of data.

IceCube is a very high-energy neutrino telescope operating at the geographic South Pole. It consists of 5,160 digital optical modules (DOMs). Each DOM contains a photomultiplier tube, supporting hardware and electronics inside a pressure glass sphere. These DOMs are arranged on 86 strings frozen into the antarctic ice at depths from 1450 m to 2450 m instrumenting one cubic kilometer. The DOMs indirectly detect neutrinos by sensing Cherenkov light produced by charged secondary particles produced in neutrino-matter interactions. A more detailed description of IceCube and its operation can be found in ref. [7].

Here we present a search for a correlation between 28 events found by IceCube using the high-energy starting event technique (HESE) and GRBs detected between May 31, 2010 and May 15, 2012. A total of 562 GRBs were reported by satellites, notably Fermi GBM and Swift BAT, in this time period [8]. All GRBs with a known trigger time and position during the two years of the HESE analysis were selected. The search reported here uses a likelihood ratio technique similar to the method used to search for neutrino point sources with IceCube [9] that relies on positional and temporal correlation between the GRB and neutrino event times and positions in the sky. Our search is able to study this correlation in timescales from $\pm$10 s to $\pm$15 days around each GRB.

2 High Energy Starting Events (HESE)

The Extremely High Energy (EHE) neutrino search and a follow-up HESE search have resulted in the first evidence of astrophysical neutrinos in IceCube [10, 11]. Because the very low rate, we can for the first time study correlations between GRBs and neutrinos over long time scales.

There are 2 main signatures for neutrinos in IceCube. Tracks are the result of deeply penetrating muons traveling for several kilometers in ice or rock at the energies relevant to IceCube. Charged current interactions of ν_μ (and a small contribution due to ν_τ) result in track-like events. Cascades, or showers, are the result of secondaries such as electrons or hadrons interacting in the ice. Neutrinos of all flavors that interact via the neutral current result in cascades. Cascades are also produced by charged current interactions of ν_e and ν_τ. For the latter flavor, a single cascade is observed if the τ decay lengths in the detector is short. Cascades have length

of a few meters and from the point of view of IceCube they can be considered as point sources of light. Track-like events have very good angular resolution, but energy can only be measured via energy deposition in the instrumented volume. Cascades have poorer angular resolution but very good visible energy resolution.

The HESE technique[11] selects neutrino-like events by vetoing events in which the earliest light is observed in the outer part of the detector. The DOMs are also required to observe a total charge of at least 6000 photo-electrons. These vetoes significantly reduce the backgrounds of down-going cosmic ray muons and through-going muons from atmospheric neutrinos. The HESE search is sensitive to neutrinos of all flavors with neutrino interaction vertices in the fiducial volume of the detector. The HESE method, and thus the search reported here, is sensitive over 4π sr. Track-like events selected by the HESE search have an angular resolution of $\approx 1^\circ$. Cascade-like events have median angular resolutions of $10-15^\circ$ and visible energy resolutions of $\approx 15\%$. The HESE technique resulted in the observation of 28 events with reconstructed energies between $\sim$30 TeV and $\sim$1.2 PeV [11]. The observations were conducted using approximately one year of full detector exposure and one year of exposure with 79 strings in operation for a total of 662 days of livetime. The background expectation is $10.6^{+4.5}_{-3.9}$ due in part to down-going muons that sneak through the veto and in part due to atmospheric neutrinos including prompt atmospheric neutrinos. This corresponds to an excess over background of 4.1 σ. Of the 28 events, 21 are cascade-like and 7 are track like. This agrees with expectations of astrophysical neutrinos and vacuum oscillations under several astrophysical scenarios [12]. No evidence of a point source of neutrinos using all 28 events or using only the 21 cascade-like events is observed [11].

3 Method

We performed a search for spatial and temporal correlations between a stacked list of 562 GRBs and the 28 HESE events. The temporal search is performed with multiple overlapping windows that increase in size by 20 s up to one day and then increase in size by 2 hours up to 15 days. The shortest time window is $\pm$10 s and the longest time window is $\pm$15 days centered at the time of each GRB. The spatial correlation is performed using detailed event by event reconstruction information. This *model independent* analysis has not been optimized for any individual predicted GRB spectra and searches for broad time and space correlations with GRBs. Our search has been constructed using blind data techniques, where event times were kept hidden during analysis preparation, and the events themselves were used to characterize the background by randomizing the times of each event.

3.1 Likelihood

For each time window ΔT from $\pm$10 s to $\pm$15 days, we define a likelihood function for the correlation of a event with a set of GRB thus:

$$\begin{aligned}\mathscr{L}_e(n_s,\Delta T) = \quad & \tfrac{n_s}{N_E} * \bar{S}_e(\theta,\phi,t,\Delta T) + \\ & \left(1-\tfrac{n_s}{N_E}\right) * B_e(\theta,\phi,t,\Delta T),\end{aligned} \tag{1}$$

where $N_E = 28$ is the number of HESE events, n_s is the unknown number of events correlated with GRBs, t is the time difference between GRB g and HESE event e, and θ and ϕ are the relative location of the GRB and the HESE event and B_g is the background (accidental correlation) probability density function (PDF). $\bar{S}_e$ is the weighted signal probability density function given by:

$$\bar{S}_e(\theta,\phi,t,\Delta T) = \frac{1}{N_G}\sum_g S_{g,e}(\theta,\phi,t,\Delta T) \tag{2}$$

where the sum is done over the signal PDF $S_{g,e}$ for all GRBs coincident with a given event e for a given time window ΔT and N_G is the number of GRBs.

The likelihood function that describes the correlation between all events and all GRBs is:

$$\mathscr{L}(n_s,\Delta T) = \prod_e \mathscr{L}_e(n_s,\Delta T) \tag{3}$$

The likelihood ratio is $\Lambda(n_s) = \mathscr{L}(n_s,\Delta T)/\mathscr{L}(n_s = 0,\Delta T)$. And the most likely value of n_s, called $\hat{n}_s$, is found by maximizing $\lambda = 2\ln(\Lambda)$ as a function of n_s for each time window ΔT. The value of λ evaluated at $\hat{n}_s$ for each time window ΔT is used as a test statistic $\hat{\lambda}(\Delta T)$.

The test statistic which is calculated for each time window is used to determine the pre-trials p-value for that time window.

3.1.1 Signal PDF

The signal PDF is composed of two parts: spatial and temporal.

$$S_{g,e}(\theta,\phi,t,\Delta T) = P_{s,g,e}(t,\Delta T)P_{s,g,e}(\theta,\phi) \tag{4}$$

The temporal component is a normalized step function based on the time window being examined. This window extends from $-\Delta T$ to $+\Delta T$ of time difference between an event e and a GRB g. Any event inside this time window has a normalized PDF value, and the signal PDF outside this window is zero.

$$P_{s,g,e}(t,\Delta T) = \begin{cases} \frac{1}{2\Delta T} & |t_e - t_g| < \Delta T \\ 0 & |t_e - t_g| > \Delta T \end{cases} \tag{5}$$

The spatial PDF of each event is based on the reconstructed likelihood map. This is a more elaborate choice than previously used for point source searches in IceCube [9]. It is necessary to use the reconstruction likelihood space for each event, specifically for cascades. Event reconstruction is performed using the time and charge of each pulse reported by the DOMs. Each reconstruction likelihood map is smoothed using the uncertainty of the GRB position as reported by the satellites and an IceCube systematic uncertainty based on the type of event (track or cascade). The smoothing is done using both uncertainties added in quadrature. GRBs reported by Fermi GBM have an uncertainty in localization of 3-10° [13], while other satellites typically localize GRBs with much better accuracy than IceCube's angular resolution. For HESE track-like events the IceCube systematic uncertainty is 1° and it is 10° for cascade-like HESE events. The smoothing also minimizes the effects of the discrete binning inherent in the reconstruction likelihood maps.

To optimize CPU usage, the smoothing is done using the Fourier transformation on the surface of a sphere of the

smoothing function and the reconstruction likelihood map [14]. After the reconstruction likelihood has been smoothed, it is normalized and a minimum floor is set 10 orders of magnitude below the peak to simplify the calculation. The information used in $P_{s,g,e}(\theta,\phi)$ is provided by the normalized and smoothed event reconstruction likelihood map. Figure 1 shows one such normalized and smoothed reconstruction likelihood.

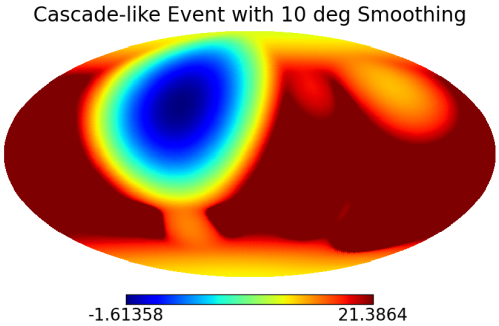

Fig. 1: Normalized Smoothed Likelihood Reconstruction Map for one of the HESE events. The map is in log space with a linear color scale. The large solid red color corresponds to the minimum likelihood value artificially put into the map.

3.1.2 Background PDF

The background PDF is also composed of temporal and spatial components.

$$B_e(\theta,\phi,t,\Delta T) = P_{b,e}(t,\Delta T)P_{b,e}(\theta,\phi), \quad (6)$$

The temporal component is given by

$$P_{b,e}(t,\Delta T) = \frac{1}{\tau}, \quad (7)$$

with $\tau = 1/\text{livetime}$. The $1/\tau$ accounts for the normalization.

The spatial component is given by

$$P_{b,e}(\theta,\phi) = \frac{1}{4\pi}. \quad (8)$$

We approximate the background PDF as $1/4\pi$. The true distribution is poorly measured since we are limited to 28 events. This approximation is reasonable since the variation scale small enough for the event spatial distribution and GRBs are known to be uniformly distributed in the sky.

3.2 Test Statistic

The test statistic gives us a measure of how signal-like a set of events is in a given time window. Since it is possible that an event and GRB could show a measure of significance by random chance, we use a Monte Carlo simulation to generate a set of scramblings to characterize the test statistic distribution for accidental coincidences.

Each scrambling is done by randomizing the event times where the event times are randomly generated from detector livetime. For this analysis we have generated 10^5 scramblings. The full set of 562 GRBs and 28 time randomized events are used to generate the likelihood ratio. For each time window in each scrambling, the likelihood ratio is maximized with respect to n_s to find $\hat{n}_s$. A larger test statistic implies a more signal-like event distribution in that time window.

For each time window, we generate a distribution of test statistics using all of the scramblings. The distribution of test statistics gives us a characterization for the test statistic assuming an accidental correlation. By comparing the test statistic for the actual event times for a given time window, we get a pre-trials p-value for that time window that indicates how signal-like the test statistic is compared to the random cases.

Figure 2 shows the test statistic distribution for $\sim 10^5$ scramblings for a time window of 100 s before and after each GRB, and figure 3 is the distribution for 10,000 s.

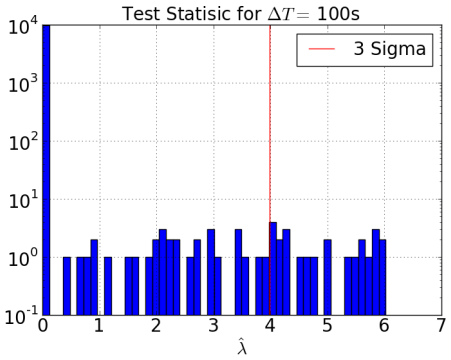

Fig. 2: Null hypothesis distribution of $\hat{\lambda}(100\text{ s})$, the test statistic for 100 s. This distribution was produced with 10^5 scramblings. The location of a 3-sigma pre-trial accidental correlation is marked by a vertical line.

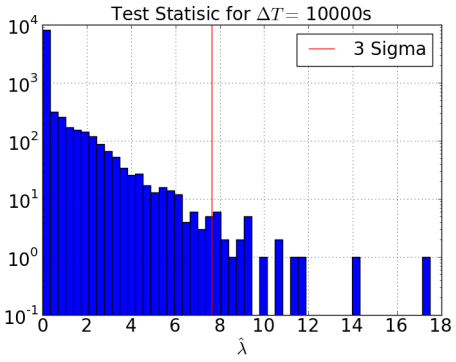

Fig. 3: Null hypothesis distribution of $\hat{\lambda}(10{,}000\text{ s})$, the test statistic for 10,000 s. This distribution was produced with 10^5 scramblings. The location of a 3-sigma pre-trial accidental correlation is marked by a vertical line.

4 Trials Factor Calculation

Since we are examining multiple overlapping time windows, we have to generate a post trials p-value. The pre-trials p-value is the significance for a set of events for a single time window, but since the time windows are not entirely independent of one another, we create a distribution of p-values based on the most significant (smallest) p-value for each scrambling.

After the test statistic distribution is generated for each time window, a p-value is determined for each time window in each scrambling. After all the p-values have been determined for a scrambling, the smallest p-value (or most extreme) for that scrambling is selected to generate a global distribution of p-values. After we have the distribution of the most significant p-values for all random scramblings, we find the most significant p-value over all time windows for the events with the unblinded times. The post trials p-value is the p-value of the most significant p-value over all time windows for the unblinded events compared to the distribution of the most significant p-values from the random scramblings. After the event times are unblinded, the post trials p-value is used to determine the significance of the events compared to the random scramblings.

5 Event Sensitivity

The Feldman Cousins 90% C.L. average upper limit [15] is calculated for each time window using the background $\mu = < \hat{n}_s(\Delta T) >$ for all scramblings. This average upper limit is our event sensitivity. It gives the upper limit on the number of events given the background μ for a null measurement. Figure 4 shows the average upper limit in each time window from 10 s to 15 days.

The average upper limit is found by taking the sum of the Feldman Cousins upper limit for n observed events with a background of μ weighted by the Poisson probability of seeing n events with background μ for all n.

$$< u.l. >= \sum_{n=0}^{\infty} P(n,\mu) * FC(n,\mu) \qquad (9)$$

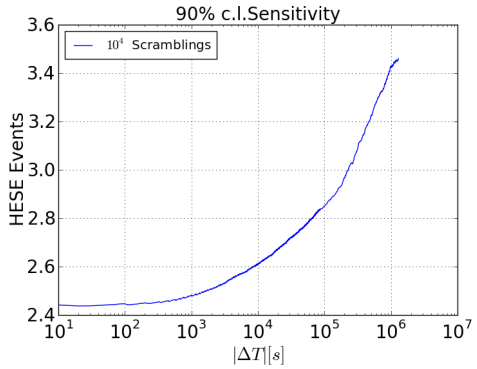

Fig. 4: Event sensitivity as a function of time window.

6 Summary

Using high energy events that interact within a fiducial volume of IceCube, we continue to probe cosmic ray production in GRBs. We focus on a model independent search over $\pm$15 days for high energy neutrinos coincident in time and space with GRBs. Due to low background rates and increased event type sensitivity, we have the opportunity to explore a previously unexamined test regime.

References

[1] Vietri M., ApJ. 453 (1995) 883-889 doi:10.1086/176448.
[2] Waxman E. & Bahcall J., Phys. Rev. Lett. 78 (1997) 2292-2295 doi:10.1103/PhysRevLett.78.2292.
[3] Waxman E. & Bahcall J., Phys. Rev. D 59 (1999) 023002 doi:10.1103/PhysRevD.59.023002.
[4] Mészáros P. & Waxman E., Phys. Rev. Lett. 87 (2001) 171102 doi:10.1103/PhysRevLett.87.171102.
[5] Abbasi, R. et al., Nature 484 (2012) 351 doi:10.1038/nature11068.
[6] Hümmer, S., Baerwald, P. & Winter, W., Phys. Rev. Lett. 108 (2012) 231101 doi:10.1103/PhysRevLett.108.231101.
[7] A. Achterberg et al., Astropart. Phys. 26 (2006) 155 doi:10.1016/j.astropartphys.2006.06.007.
[8] Aguilar, J.-A., arXiv:1110.5946 (2011) and references therein.
[9] Braun J. et al., Astropart. Phys. 29 (2008) 299-305 doi:10.1016/j.astropartphys.2008.02.007.
[10] M. G. Aartsen et al., arXiv:1304.5356 (2013).
[11] IceCube Coll., paper 0650 these proceedings.
[12] Kashti T. & Waxman E. Phys. Rev. Lett. 95 (2005) 181101 doi:10.1103/PhysRevLett.95.181101.
[13] Paciesas, W. S. et al., Astropart. Phys. 199 (2006) 18.
[14] Baddour, N. J., Opt. Soc. AM. A 27 (2010) 2144 doi:10.1364/JOSAA.27.002144.
[15] Feldman, G. & Cousins, R. Phys. Rev. D 57 (1998) 3873 doi:10.1103/PhysRevD.57.3873.